Electronic Supplementary Material (ESI) for Nanoscale.

Supporting Information

Self-Supporting $Ti_3C_2T_x$ Foam/S Cathodes with High Sulfur Loading for High-Energy-Density Lithium−Sulfur Batteries

Tongkun Zhao,[a] *Pengfei Zhai,*[a] *Zhihao Yang,*[a] *Junxiao Wang,*[a] *Lingbo Qu,*[b] *Fengguang Du,*[b] *Jingtao Wang**[a]

[a] School of Chemical Engineering and Energy, Zhengzhou University, Zhengzhou 450001, P. R. China

[b] State Key Laboratory of Motor Vehicle Biofuel Technology, Nanyang 473000, P.R. China

*To whom correspondence should be addressed.

Fax: +86-371-63887135; Tel: +86-371-63887135; E-mail: jingtaowang@zzu.edu.cn

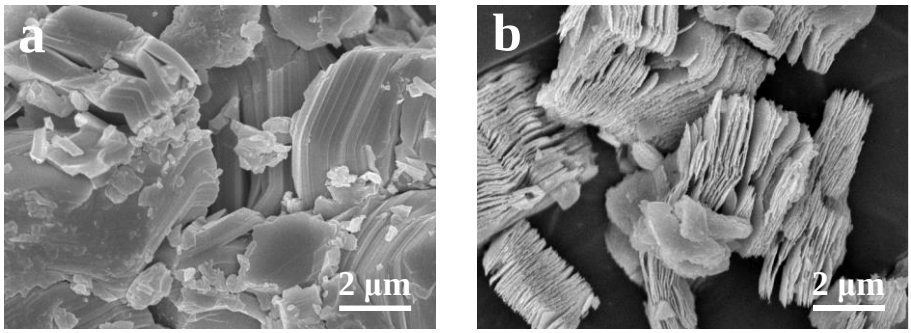

Fig. S1. SEM images of (a) Ti_3AlC_2 particle and (b) $Ti_3C_2T_x$ powder.

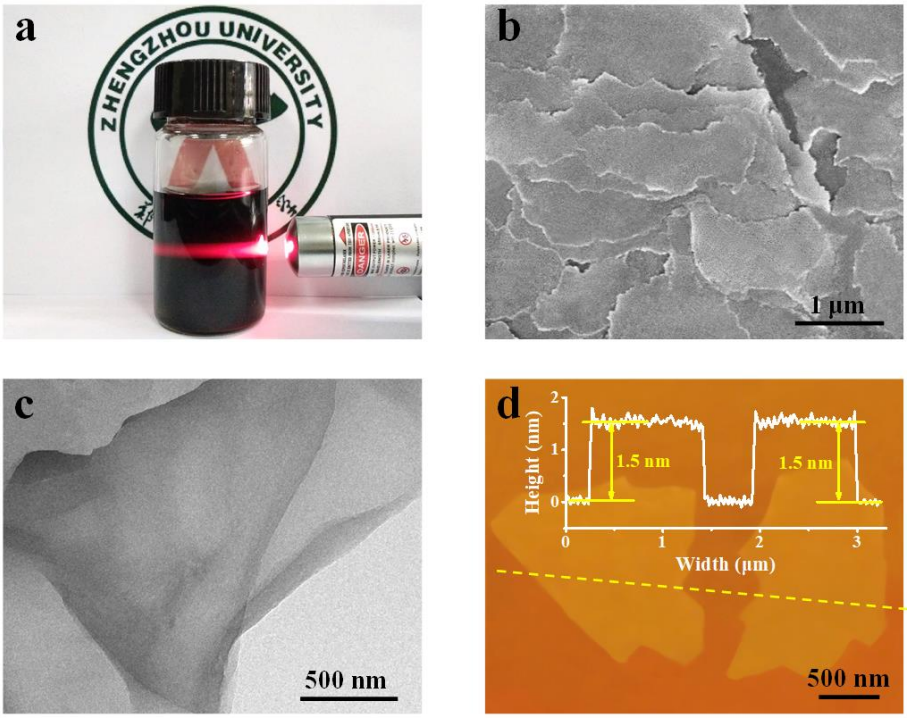

Fig. S2. (a) The optical image of the $Ti_3C_2T_x$ colloidal suspension and the corresponding Tyndall effect; (b) SEM image, (c) TEM image and (d) AFM image of the $Ti_3C_2T_x$ flakes.

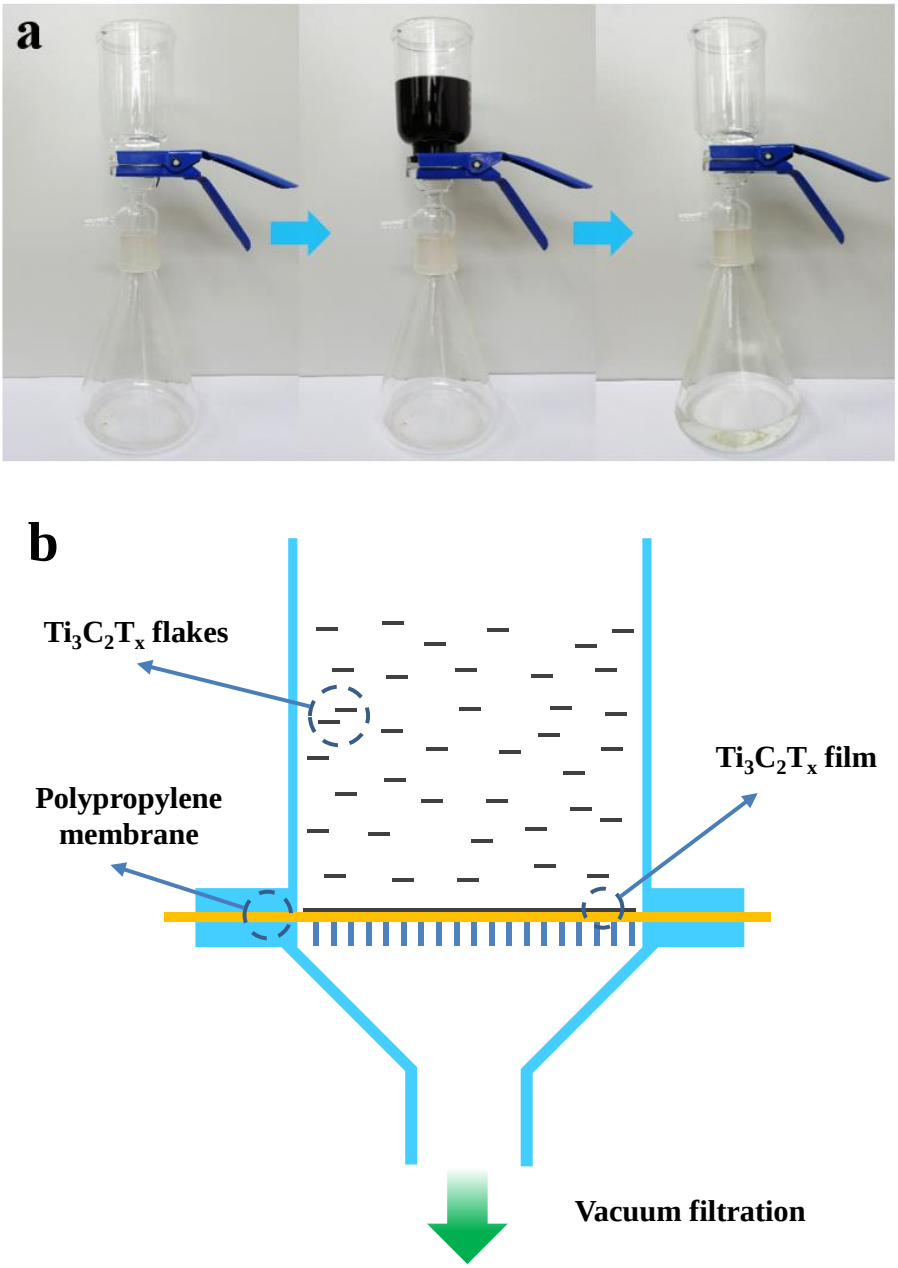

Fig. S3. Preparation of the $Ti_3C_2T_x$ film by simple vacuum-assisted filtration: (a) the optical images and (b) schematic illustration for the vacuum-assisted filtration process.

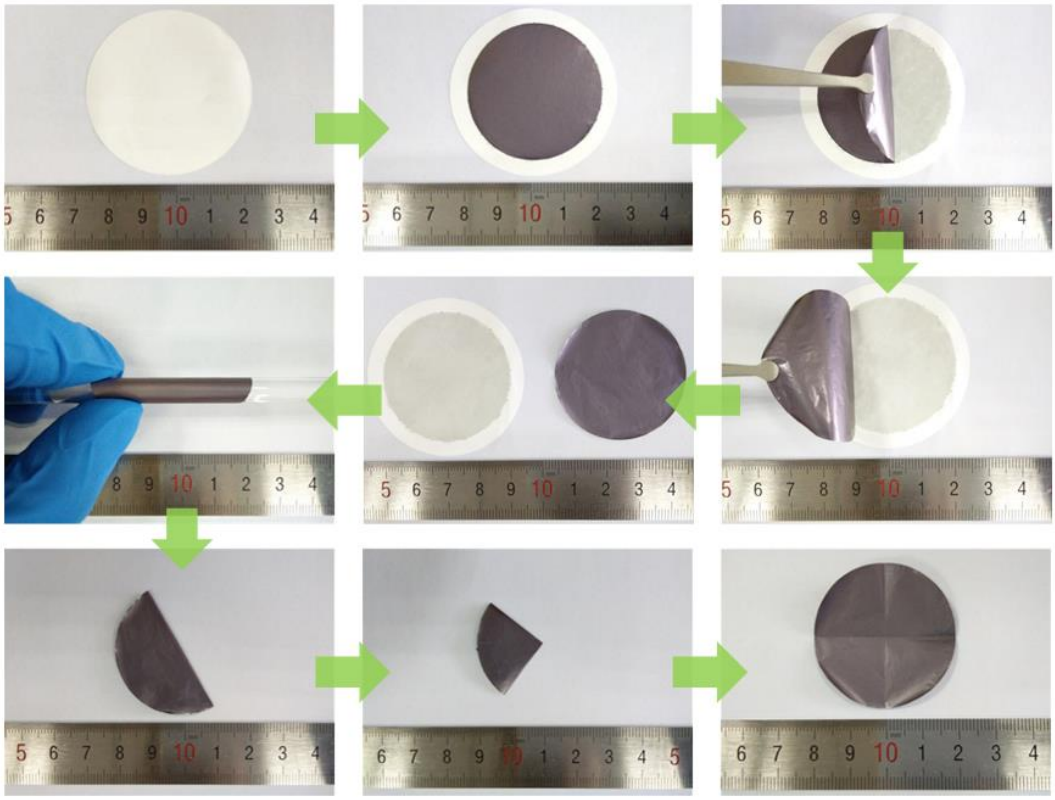

Fig. S4. The photographs of the freestanding $Ti_3C_2T_x$ film peeled from the polypropylene membrane and good flexibility exhibition.

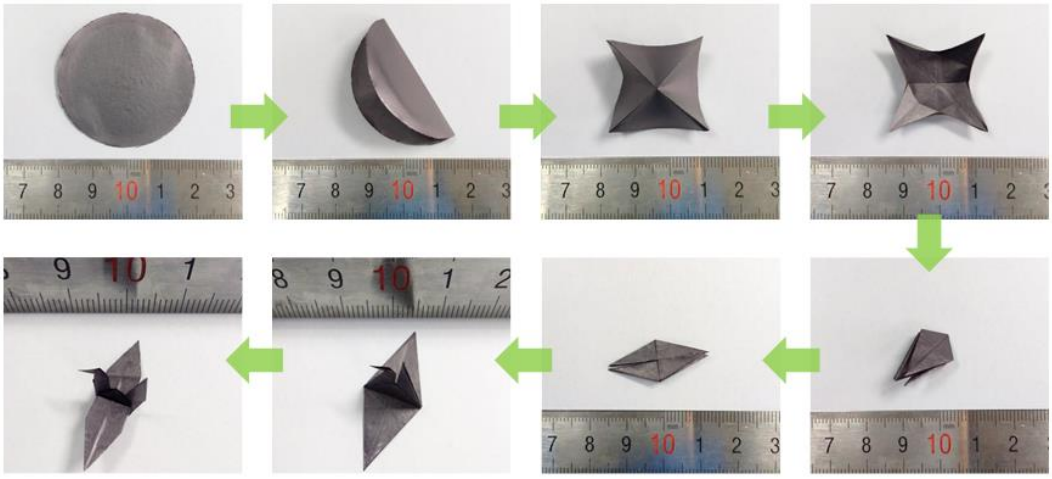

Fig. S5. The photographs of mechanical stability and flexibility exhibition of $Ti_3C_2T_x$ film.

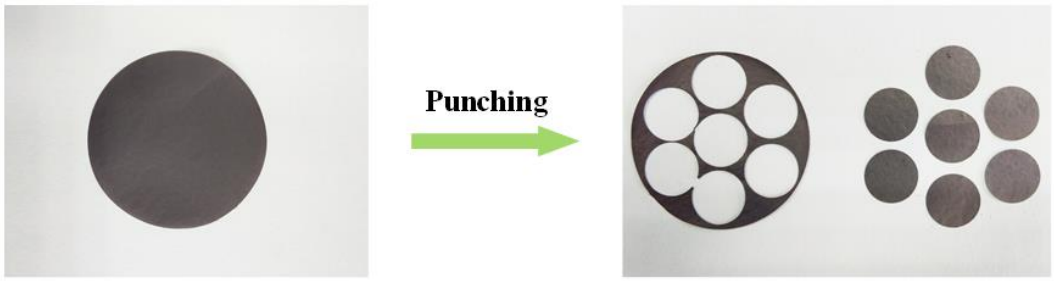

Fig. S6. The photographs for the $Ti_3C_2T_x$ film punched into discs with a diameter of 12 mm.

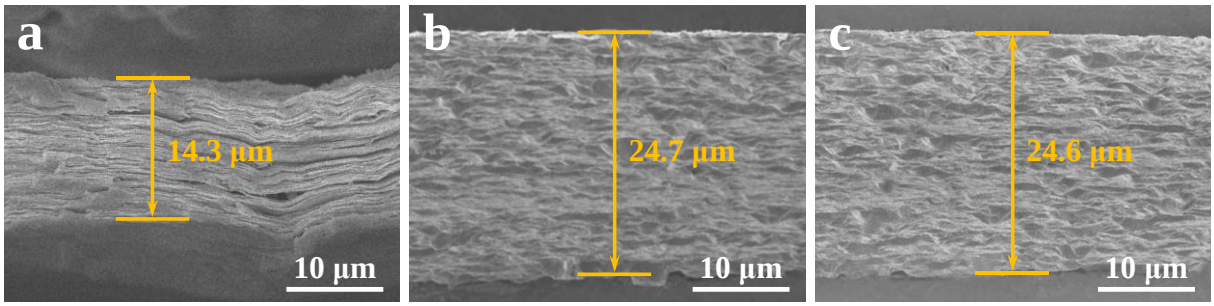

Fig. S7. Cross-sectional SEM images of (a) $Ti_3C_2T_x$ film, (b) $Ti_3C_2T_x$ foam, and (c) $Ti_3C_2T_x$ foam/S-1.5. Note that both (b) $Ti_3C_2T_x$ foam and (c) $Ti_3C_2T_x$ foam/S-1.5 are derived from the same (a) $Ti_3C_2T_x$ film.

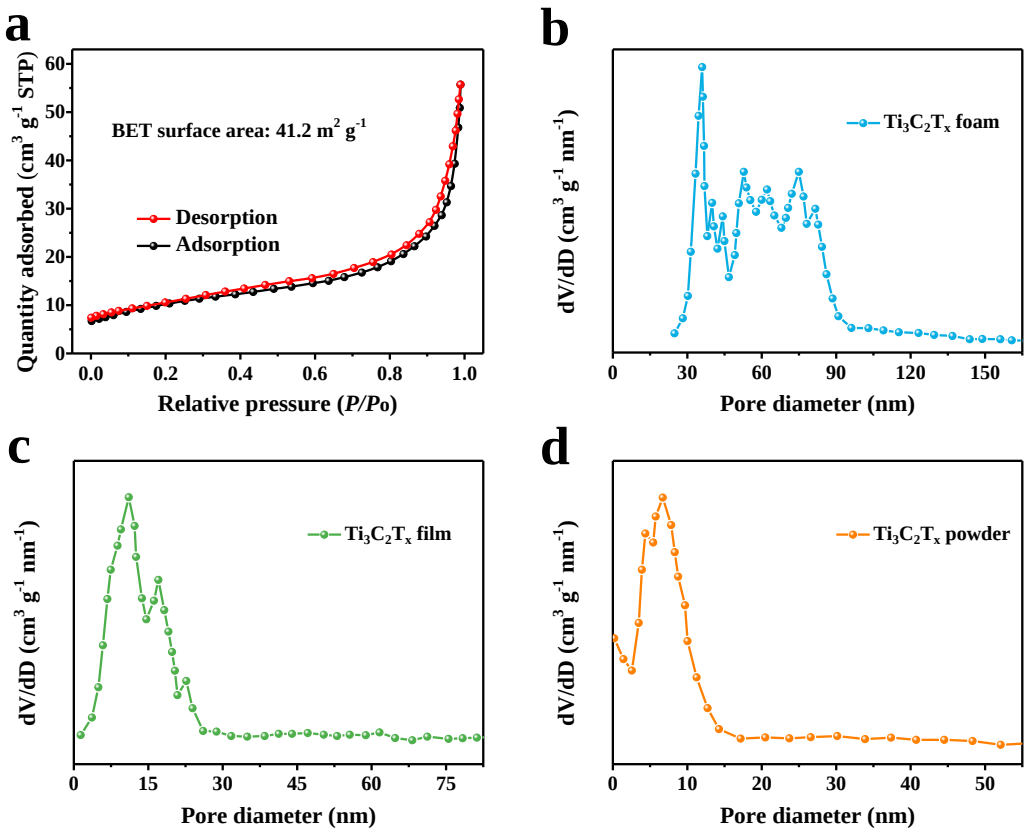

Fig. S8. (a) N_2 adsorption–desorption isotherms of the $Ti_3C_2T_x$ powder; The pore size distributions of (b) $Ti_3C_2T_x$ foam, (c) $Ti_3C_2T_x$ film, and (d) $Ti_3C_2T_x$ powder.

Fig. S9. The photographs for the long-term durability and stability of the $Ti_3C_2T_x$ foam in electrolyte.

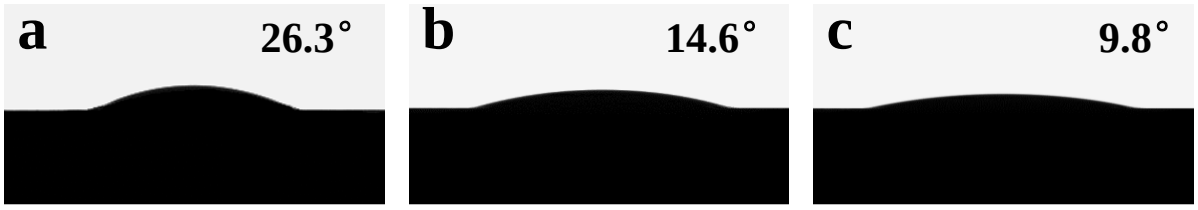

Fig. S10. Contact angle measurement between electrolyte and (a) $Ti_3C_2T_x$ powder, (b) $Ti_3C_2T_x$ film, and (c) $Ti_3C_2T_x$ foam.

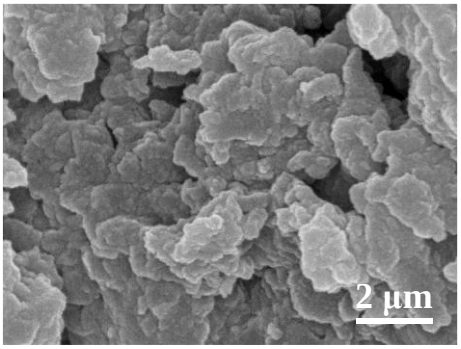

Fig. S11. SEM image of the $Ti_3C_2T_x$/S composite.

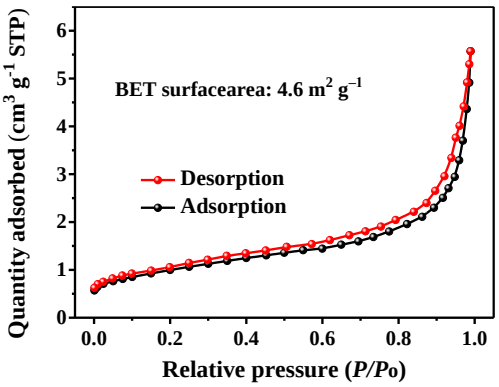

Fig. S12. N_2 adsorption–desorption isotherms of the $Ti_3C_2T_x$ foam/S-1.5.

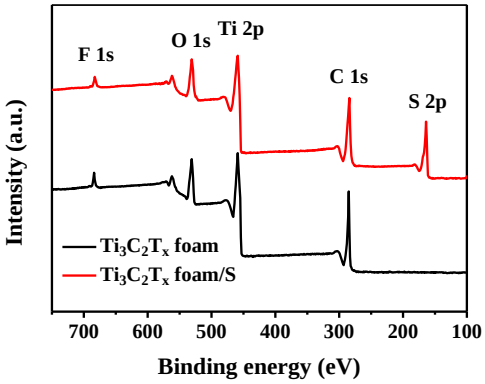

Fig. S13. XPS survey spectra of the $Ti_3C_2T_x$ foam and $Ti_3C_2T_x$ foam/S.

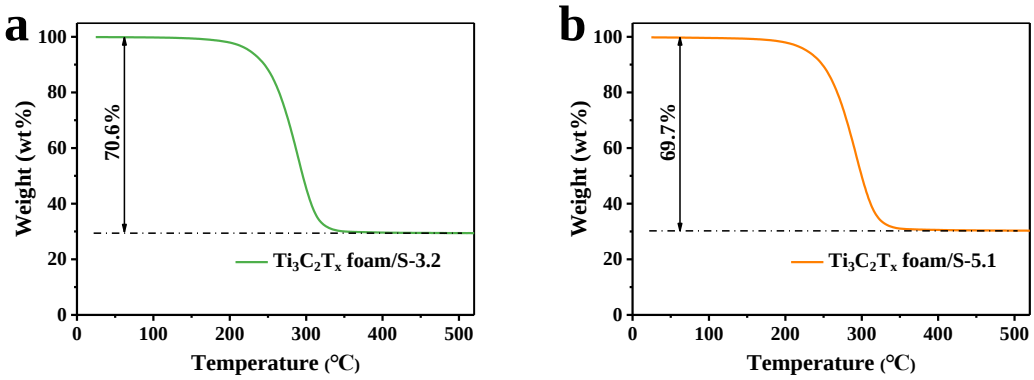

Fig. S14. TGA curves of (a) $Ti_3C_2T_x$ foam/S-3.2 and (b) $Ti_3C_2T_x$ foam/S-5.1.

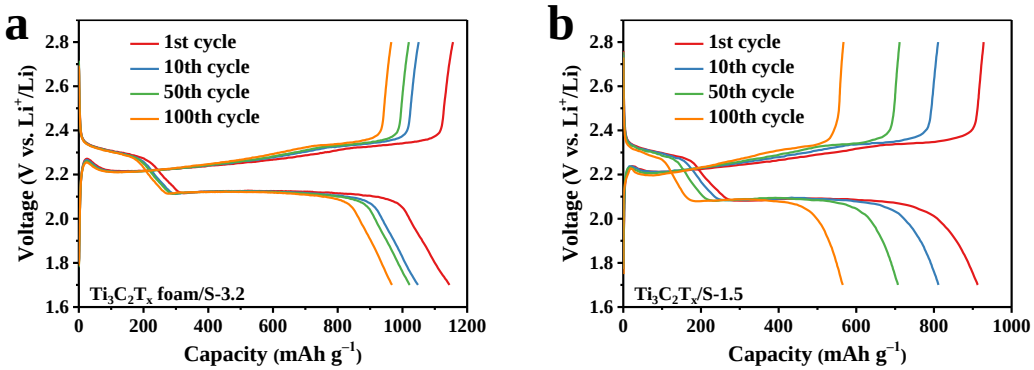

Fig. S15. Charge/discharge curves of (a) $Ti_3C_2T_x$ foam/S-3.2 and (b) $Ti_3C_2T_x$/S-1.5 cathodes at 0.2 C.

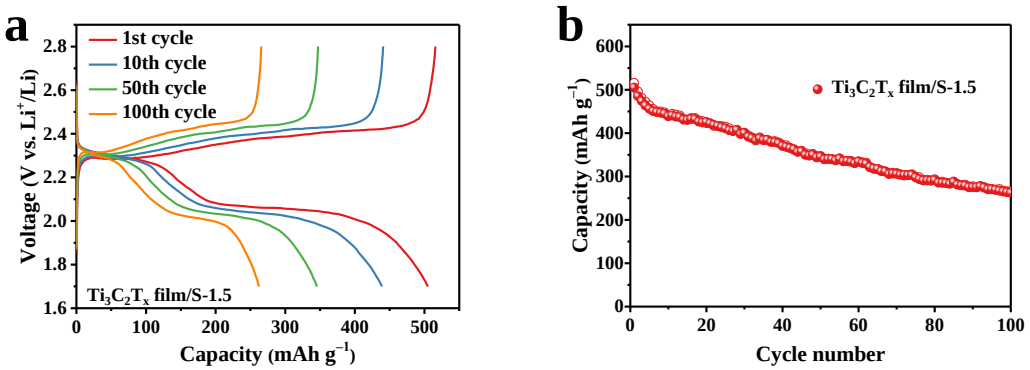

Fig. S16. (a) Charge/discharge curves and (b) cycling performance of $Ti_3C_2T_x$ film/S-1.5 cathode at 0.2 C.

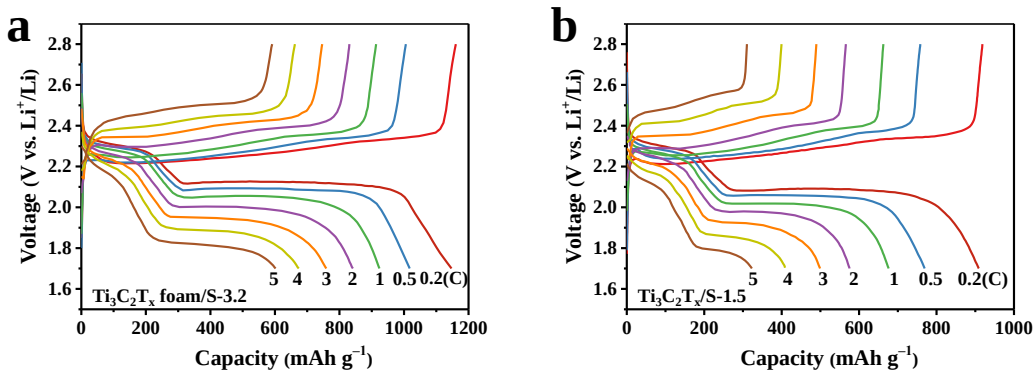

Fig. S17. Charge/discharge curves of (a) $Ti_3C_2T_x$ foam/S-3.2 and (b) $Ti_3C_2T_x$/S-1.5 cathodes at various rates.

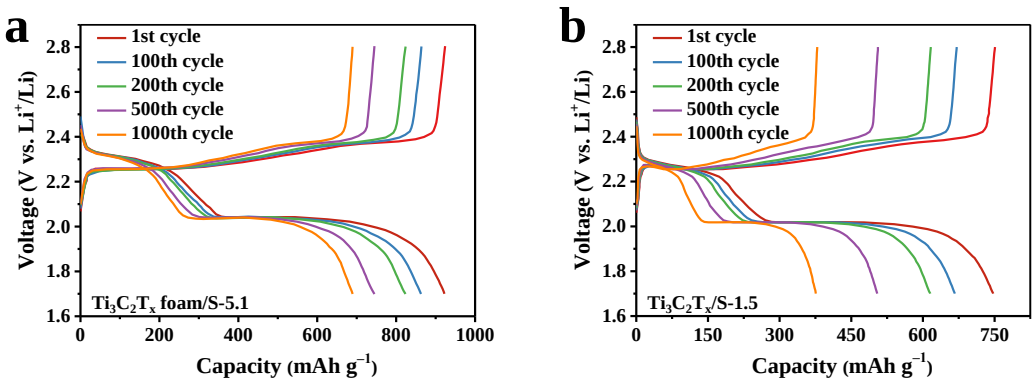

Fig. S18. Charge/discharge curves of (a) $Ti_3C_2T_x$ foam/S-5.1 and (b) $Ti_3C_2T_x$/S-1.5 cathodes at 1 C.

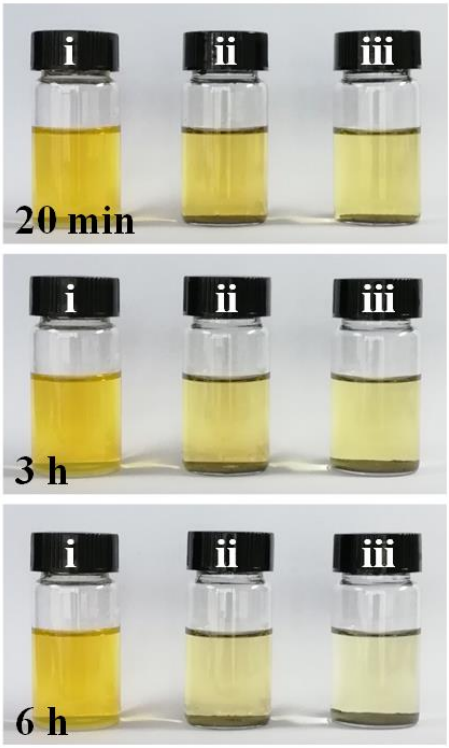

Fig. S19. The optical photographs of (i) the pristine Li_2S_6, (ii) Li_2S_6+$Ti_3C_2T_x$, and (iii) Li_2S_6+$Ti_3C_2T_x$ foam solution after keeping for 20 min, 3 h, and 6 h, respectively.

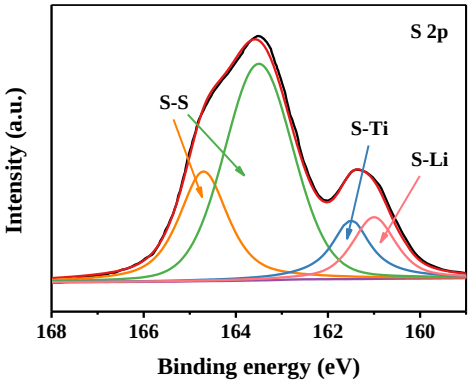

Fig. S20. S 2p XPS spectrum of the $Ti_3C_2T_x$ foam adsorbed with Li_2S_6.

Table S1. Summary of relative parameters of various cathodes in this work.

Cathode	m(S)/mg	m(c)/mg	m(Al)/mg	m(t)/mg
$Ti_3C_2T_x$ foam/S-1.5	1.70	2.39	0	2.39
$Ti_3C_2T_x$ foam/S-3.2	3.62	5.13	0	5.13
$Ti_3C_2T_x$ foam/S-5.1	5.76	8.26	0	8.26
$Ti_3C_2T_x$/S-1.5	1.70	3.25	2.82	6.07

Table S2. Summary of energy density of various cathodes based on the mass of sulfur m(S).

Cathode	$E_{m(S)}$/Wh kg^{-1}						
	0.2 C	0.5 C	1 C	2 C	3 C	4 C	5 C
$Ti_3C_2T_x$ foam/S-1.5	1824.5	1634.9	1473.0	1326.9	1190.8	1068.2	954.4
$Ti_3C_2T_x$ foam/S-3.2	1703.5	1500.6	1344.9	1200.0	1061.0	922.8	802.7
$Ti_3C_2T_x$ foam/S-5.1	1567.9	1358.9	1212.9	1077.1	937.2	800.0	673.6
$Ti_3C_2T_x$/S-1.5	1337.7	1121.7	974.9	817.8	695.3	558.1	433.6

Table S3. Summary of energy density of various cathodes based on the total mass of cathode m(t).

Cathode	$E_{m(t)}$/Wh kg^{-1}						
	0.2 C	0.5 C	1 C	2 C	3 C	4 C	5 C
$Ti_3C_2T_x$ foam/S-1.5	1297.8	1162.9	1047.7	943.8	847.0	759.8	678.9
$Ti_3C_2T_x$ foam/S-3.2	1202.1	1058.9	949.0	846.8	748.7	651.2	566.4
$Ti_3C_2T_x$ foam/S-5.1	1093.4	947.6	845.8	751.1	653.5	557.9	469.7
$Ti_3C_2T_x$/S-1.5	374.6	314.1	273.0	229.0	194.7	156.3	121.4

where *m(S)* is the mass of sulfur in cathode, *m(c)* is the mass of cathode without Al current collector, *m(Al)* is the mass of Al current collector, *m(t)* is the total mass of cathode, $E_{m(S)}$ is energy density based on the mass of sulfur *m(S)*, and $E_{m(t)}$ is energy density based on the total mass of cathode *m(t)*. Note that the $E_{m(S)}$ values are collected from the LAND CT2001A battery tester, and the $E_{m(t)}$ values are calculated by equation of $E_{m(t)} = E_{m(S)} \times m(S) / m(t)$.